J. Fluid Mech. (1987), *vol.* 174, *pp.* 553–563
Printed in Great Britian

On the spatial instability of piecewise linear free shear layers

By T. F. BALSA

Aerospace and Mechanical Engineering Department, University of Arizona, Tucson, AZ 85721, USA

(Received 16 June 1986)

The main goal of this paper is to clarify the spatial instability of a piecewise linear free shear flow. We do this by obtaining numerical solutions to the Orr–Sommerfeld equation at high Reynolds numbers. The velocity profile chosen is very much like a piecewise linear one, with the exception that the corners have been rounded so that the entire profile is infinitely differentiable. We find that the (viscous) spatial instability of this modified profile is virtually identical to the *inviscid* spatial instability of the piecewise linear profile and agrees qualitatively with the inviscid results for the tanh profile when the shear layers are convectively unstable. The unphysical features, previously identified for the piecewise linear velocity profile, arise only when the flow is absolutely unstable. In a nutshell, we see nothing wrong with the inviscid spatial instability of piecewise linear shear flows.

1. Introduction

With the use of high-speed digital computers, the calculation of the spatial eigenvalues of the Orr–Sommerfeld equation is a reasonably straightforward task, although not necessarily without difficulties. Such calculation usually leads to several different curves of spatial instability in complex wavenumber space, k, along which $\omega_R = \mathrm{Re}(\omega) \equiv 0$, where $\omega = \omega(k)$ is the dispersion relation (Huerre & Monkewitz 1985 figure 3*b*). [Note the modal time dependence is of the form $\exp(\omega t)$; $\mathrm{i} = (-1)^{\frac{1}{2}}$ is omitted from the exponent.] In order to determine which of these spatial instability curves is relevant physically, the initial value problem must be solved; typically this involves the use of Fourier transforms and certain contour deformations in complex wavenumber space. In order to carry out these deformations with reasonable certainty and rigour, the dispersion relation (its singularities, behaviour at infinity, etc.) must be known for all complex wavenumbers; the obvious limitation of any numerical approach is then immediately apparent.

Clearly what is needed, at least in model problems, is an analytic expression for the dispersion relation, and this can usually be obtained for highly idealized velocity profiles consisting of straight line segments. Rayleigh himself examined the temporal instability of a piecewise linear shear flow (figure 1) in the inviscid limit (Rayleigh 1945 p. 392) and concluded that 'diminution of wave-length below a certain value is accompanied by an instability which gradually decreases, and is finally exchanged for actual stability'. The stability to which Rayleigh is referring is precisely neutral (i.e. zero growth rate), and at the neutral point, the dispersion relation exhibits a square-root behaviour (and this implies the presence of a branch cut in k space).

One of the questions that we answer in this paper is the extent to which these observations remain unaltered by the inclusion of viscosity and finite curvatures in the velocity profile, localized to the edges of the shear layer.

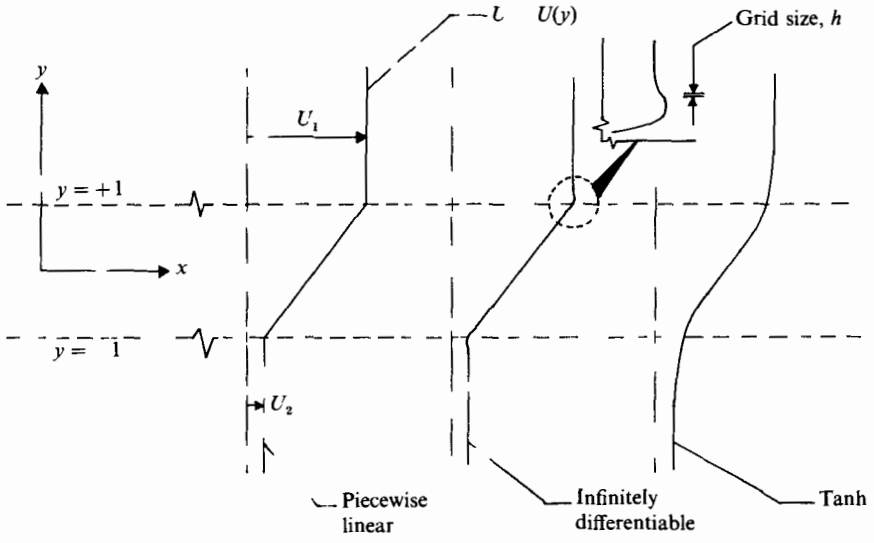

FIGURE 1. Geometry of shear layer and base velocity profiles. (The inset shows the small overshoot associated with the infinitely differentiable profile).

Esch (1957), presumably inspired by the simplicity of the piecewise linear profile and the novelty of digital computing, carried out a combined theoretical and numerical effort to understand the viscous (temporal) instability of this shear layer. Later, we shall have an occasion to make a direct comparison with his results which, unfortunately, are restricted to growing disturbances.

Bechert (1972) examined the spatial instability of a piecewise linear shear layer in the inviscid limit. He obtained some curious results which are quite different from what might be expected for smoothly varying profiles on the basis of the results of Michalke (1965).

The second issue which we address in this paper centres around the high Reynolds-number spatial instability of a near piecewise linear shear layer whose corners have been slightly rounded so that the profile is infinitely smooth. Through numerical solutions of the Orr–Sommerfeld equation, we establish that the spatial instability of this profile is quite meaningful when the flow is convectively unstable. The resemblance of this spatial instability to that of the inviscid piecewise linear profile is remarkable. Finally, we re-examine the Bechert results and explain why they are completely misleading.

2. Relevant equations

The central equation of linear and parallel flow stability theory is the Orr-Sommerfeld equation (Drazin & Reid 1982 p. 156),

$$(U-c)\,\mathrm{D}\phi - U''\phi = \frac{1}{\mathrm{i}k}\frac{1}{Re}\,\mathrm{D}^2\phi, \tag{1a}$$

where

$$\mathrm{D} = \frac{\mathrm{d}^2}{\mathrm{d}y^2} - k^2, \quad U'' = \frac{\mathrm{d}^2 U}{\mathrm{d}y^2}, \tag{1b}$$

and $\phi = \phi(y)$ represents the cross-space structure of the y velocity component

$$v(x, y, t) = \mathrm{e}^{\omega t}\,\mathrm{e}^{\mathrm{i}kx}\,\phi(y). \tag{1c}$$

Here, $k = (k_R, k_I)$ denotes the complex wavenumber, $\omega = \omega(k)$ is the (complex) dispersion relation, $c = i\omega/k$ is the (complex) eigenvalue, and Re and $U = U(y)$ denote the Reynolds number and the base velocity profile, respectively. The geometry of the shear layer is shown in figure 1. The Rayleigh equation is recovered from the Orr–Sommerfeld equation by setting the right-hand side of (1*a*) to zero (i.e. $Re = \infty, k \neq 0$ fixed).

It remains to specify the base velocity profiles, $U = U(y)$, and we shall consider the following three free-shear-layer flows with uniform external streams U_1 and U_2 (without loss of generality, we take $U_1 \geqslant U_2$):

Piecewise linear profile (a profile of Rayleigh)

$$U(y) = \begin{cases} U_1 = \text{const} & (y \geqslant 1), \\ U_m(1+Ry) & (|y| \leqslant 1), \\ U_2 = \text{const} & (y \leqslant -1). \end{cases} \tag{2a}$$

Infinitely differentiable profile

$$U(y) = U_m[1 + RF(y)], \tag{2b}$$

where $F(y)$ is an infinitely differentiable odd function of y such that for $y \geqslant 0$ we have

$$F(y) = \begin{cases} y & (y \leqslant 1-\epsilon), \\ \frac{1}{2}\xi\left(1 - \tanh\frac{\xi}{\epsilon^2 - \xi^2}\right) + 1 & (|\xi| \leqslant \epsilon), \\ 1 & (y \geqslant 1+\epsilon), \end{cases} \tag{2c}$$

with $\xi = y - 1$. The point is that (2*b*,*c*) approximate the piecewise linear profile (2*a*), arbitrarily closely as $\epsilon \to 0$, yet (2*b*) is infinitely smooth (in our calculations we set $\epsilon = 0.3$).

Of course, one of the key issues of this paper centres around the high-Reynolds-number spatial instability of the infinitely differentiable profile and the extent to which this instability can be reproduced by the inviscid results for the piecewise linear profile. Finally, for purposes of qualitative comparisons, we also examine the instability of the tanh profile.

Tanh profile

$$U(y) = U_m(1 + R\tanh y), \tag{2d}$$

where $U_m = \frac{1}{2}(U_1 + U_2) = U(0), \Delta U = U_1 - U_2 \geqslant 0$, and $R = \Delta U/2U_m$ are the shear-layer mean velocity, velocity difference, and velocity ratio, respectively. For each velocity profile, the vorticity thickness is 2.

These three velocity profiles are also shown in figure 1 for the velocity ratio $R = 0.75$.

3. Discussion of results

In order to provide a familiar starting point for our discussion, we quote the inviscid dispersion relation for the piecewise linear profile (Rayleigh 1945 p. 393)

$$\omega(k) = -ikU_m \pm \frac{\Delta U}{4}[e^{-4k} - (1-2k)^2]^{\frac{1}{2}}, \tag{3}$$

where the $\pm$ sign is associated with the unstable and stable modes once a suitable branch for the square root has been specified. [Note that (3) is a slight extension of the Rayleigh result and it is valid for $k_R \geqslant 0$.]

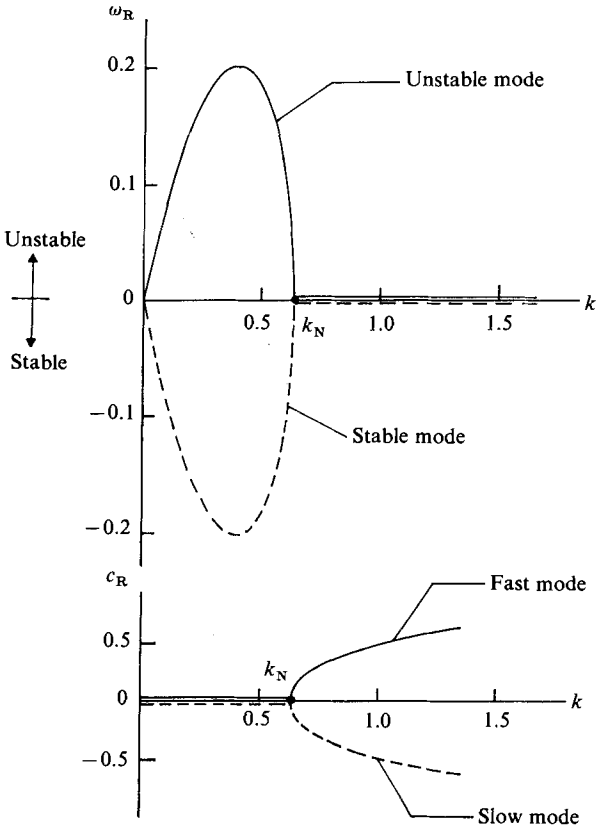

FIGURE 2. Inviscid temporal instability of piecewise linear profile: growth rate (ω_R) and phase speed (c_R) as function of wavenumber k ($U_1 = 1$, $U_2 = -1$).

3.1. *Temporal instability* ($U_1 = 1, U_2 = -1$)

Although our main interest is in spatial instabilities, it is necessary to say a few words about temporal instabilities because the former are simply the analytic continuations of the latter into the complex wavenumber plane. We therefore begin with the temporal growth rate, $\omega_R = \mathrm{Re}(\omega)$, and the phase speed, $c_R = \mathrm{Re}(c)$, for the piecewise linear profile in the inviscid limit (figure 2). These well-known results come from (3). The unstable mode basically exemplifies the kind of free-shear-flow instability that we have in mind.

A most important characteristic of these results is the existence of a neutral point at $k = k_N \approx 0.6392$. This neutral point is also a square-root branch point (i.e. $k_N = k_B$) as necessarily implied by the coalescence of the unstable and stable modes. Beyond the neutral point (i.e. for $k > k_N$), the flow is precisely neutral and the shear layer sustains a fast mode ($U_m \leqslant c_R \leqslant U_1$) and a slow mode ($U_2 \leqslant c_R \leqslant U_m$). Because of the existence of a branch point at $k = k_B$, we must have a branch cut in the complex wavenumber space; in fact, the branch cut extends from $k_B \approx 0.6392$ to plus infinity along the real axis.

We now come to one of the central questions of this paper: To what extent are these observations on the inviscid instability of the piecewise linear profile robust in the sense that these observations still survive after the inclusion of viscosity and finite curvatures of the base velocity profile (in the vicinity of $y = \pm 1$)?

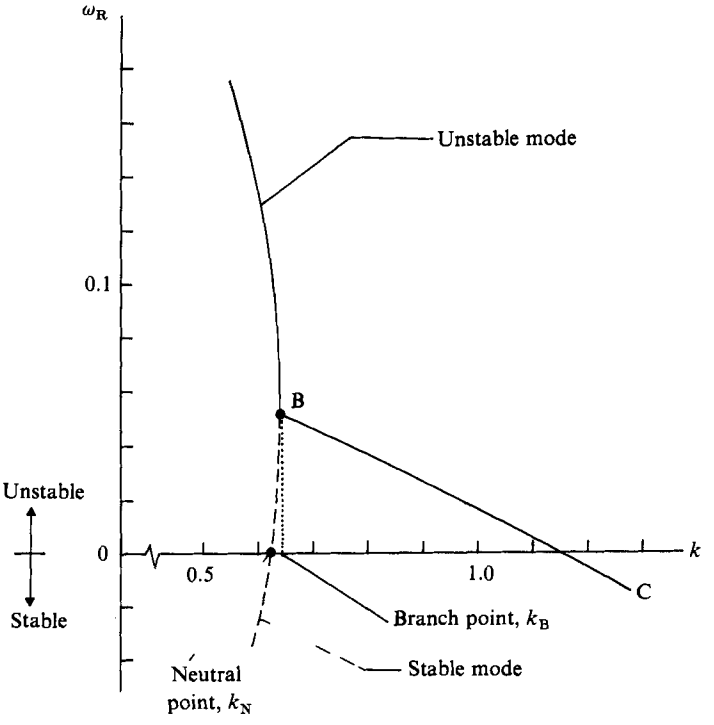

FIGURE 3. Temporal instability of infinitely differentiable profile: growth rate (ω_R) as a function of wavenumber k. $Re = 100$, $U_1 = 1$, $U_2 = -1$.

In order to answer this question, we obtained highly accurate numerical solutions to the Orr–Sommerfeld equation for the infinitely differentiable base velocity profile at various Reynolds numbers. The grid size ($h = 8 \times 10^{-3}$) used in our calculations is small enough to resolve both the viscous critical layers and the details associated with the small overshoot (less than 1 % in magnitude; see figure 1).

A typical result for the temporal growth rate at $Re = 100$ is shown in figure 3. We once again find a branch point on the real axis (at $k = k_B$), although the branch and neutral points are usually distinct. In fact, in this example, the neutral point, $k = k_N$, represents the wavenumber at which a stable mode becomes unstable (rather than the place at which the unstable mode becomes stable). We have used several different techniques to verify that $k = k_B$ is indeed a square-root branch point and that the branch cut once again extends along the real axis from k_B to plus infinity. To the right of the branch point, the growth rate is given by curve BC and the phase speeds are $c_R = U_m \pm \delta(k)$ for some numerically determined function $\delta = \delta(k)$. The $\pm$ sign in the last equation essentially corresponds to the fast and slow modes of figure 2. To the left of k_B, the instability waves are non-dispersive with $c_R = U_m$.

Furthermore, in our studies we have identified a square-root branch point on the real axis at all Reynolds numbers, even as low as $Re = 25$. In general, k_N and k_B are quite close to each other, although sometimes the point B (see figure 3) lies below the real axis (e.g. at $Re = 25$). In any case, for $Re > 1000$, the branch and neutral points are virtually indistinguishable.

The Orr–Sommerfeld results for the infinitely differentiable base velocity profile clearly indicate that the square-root behaviour of dispersion relation (3) [i.e. $\omega \sim (k - k_B)^{\frac{1}{2}}$] is totally unrelated to the piecewise nature of the base velocity profile

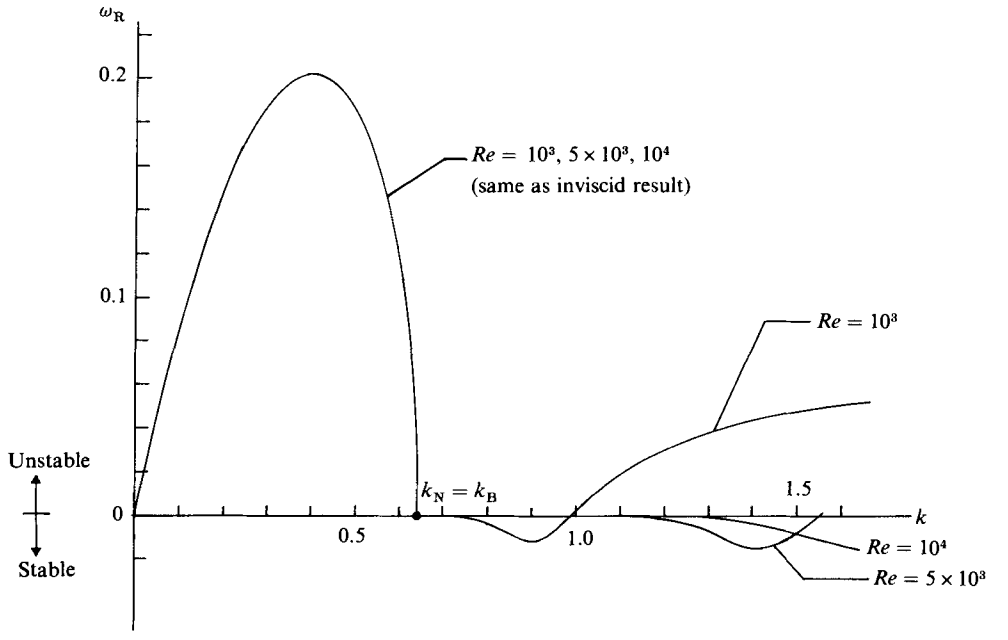

FIGURE 4. Temporal instability of infinitely differentiable profile: growth rate (ω_R) as a function of wavenumber (k) for several values of Reynolds number Re ($U_1 = 1$, $U_2 = -1$).

or to any unphysical feature arising from the Rayleigh equation. This square-root behaviour is a generic result which will occur whenever the base velocity is sufficiently linear near the shear-layer centreline at $y = 0$. [The significance of $y = 0$ is that the base velocity is antisymmetric about this point so that the phase velocity of the unstable mode is $c_R = U(0) = U_m$.]

Next, let us look at the temporal instability of the infinitely differentiable profile for $k > k_N$ ($= k_B$) and at large Reynolds numbers. Some representative results are shown in figure 4. Interestingly enough, for this range of wavenumbers, the shear flow may be stable or unstable, although on physical grounds we certainly expect the flow to be stable as $k \to \infty$. On the other hand, our calculations strongly suggest that as $Re \to \infty$, $\omega_R \equiv 0$ at all finite wavenumbers beyond the neutral point. In other words, the critical wavenumber at which the growth rate first departs significantly from zero can be exiled to infinity by letting the Reynolds number approach infinity.

These solutions of the Orr–Sommerfeld equation for the infinitely differentiable profile imply that an unstable mode for $k < k_N$ will become precisely neutral for $k > k_N$ when the Reynolds number is high enough. This conclusion, together with the one on the square-root behaviour of the dispersion relation, strongly suggests that the inviscid results for the piecewise linear profile (figure 2) are physically meaningful at all finite wavenumbers. Thus, these inviscid results are robust and remain unaltered by the inclusion of a small amount of viscosity and finite curvature of the base velocity at the edges of the shear layer! This conclusion will be reconfirmed by detailed comparisons for spatial instability.

We digress, however, for a moment to compare our results with those of Esch (1957). Esch calculated the viscous instability of the piecewise linear profile, and his results for the neutral wavenumber (as a function of Reynolds number) are shown in figure 5. The good agreement between our calculations for the infinitely differen-

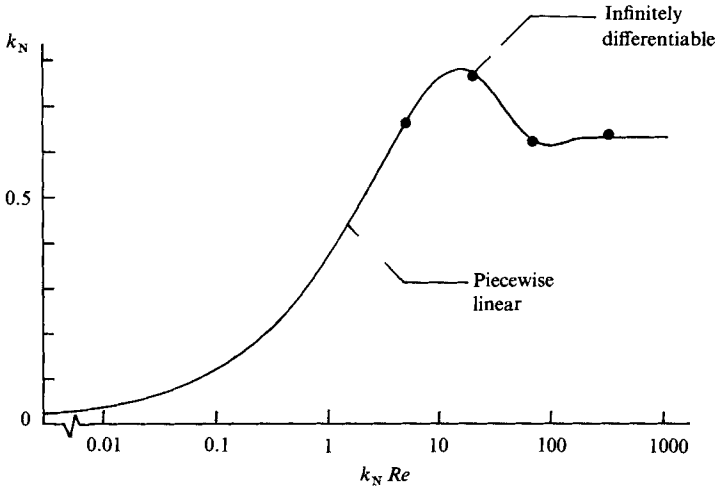

FIGURE 5. Neutral wavenumber k_N as a function of Reynolds number; $U_1 = 1$, $U_2 = -1$. —, Esch (1957); ●, present results.

tiable profile and Esch's results for the piecewise linear profile implies that the finite curvature of the base velocity profile at the edges of the shear layer has negligible influence on the basic instability of the shear layer arising from the velocity difference $\Delta U = U_1 - U_2$ across the layer.

3.2. *Spatial Instability* ($U_m = 0.5$)

Although the results for temporal instability were given for a specific shear layer with $U_1 = 1$, $U_2 = -1$, our conclusions are valid for any values of the external streams since temporal instability is Galilean invariant (of course, spatial instability is not). For our purposes, it is convenient to think of spatial instability as a curve in the complex wavenumber plane. Along this curve, $\omega_R = \mathrm{Re}(\omega) = 0$ and the frequency, $\omega_I = \mathrm{Im}(\omega)$, varies in some manner. The spatial growth rate is $-k_I$.

A typical result for the spatial instability of the infinitely differentiable profile is shown in figure 6 for a large Reynolds number. The curve of spatial instability, along which the frequency increases monotonically, originates at $k = 0$, proceeds to the right, and eventually intersects the branch cut at $k = k_S > k_N$. Along the branch cut, the spatial growth rate is zero. The existence of a branch cut can be clearly sensed by plotting neighbouring curves, say $\omega_R = \pm 0.01$. The agreement between these numerical results and the inviscid results for the piecewise linear profile, shown as dots in figure 6 [see (3)], is truly remarkable. This suggests very convincingly that the classical results of Rayleigh duplicate all aspects of the viscous, high-Reynolds-number (i.e. $Re \to \infty$) spatial instability of our infinitely differentiable velocity profile at finite wavenumbers (see also figure 4).

For reference, in figure 7, we show the curve of spatial instability for the tanh profile. This curve is very similar in the unstable range ($k_I < 0$) to the one for the infinitely differentiable profile (figure 6). At wavenumbers corresponding to stability ($k_I \geqslant 0$), disturbances in the tanh profile are damped whereas those in the infinitely differentiable profile are exactly neutral. This latter difference between these two shear layers is very interesting mathematically, but physically it is quite insignificant since damped or neutral modes usually do not play an important role in a shear layer that is violently unstable.

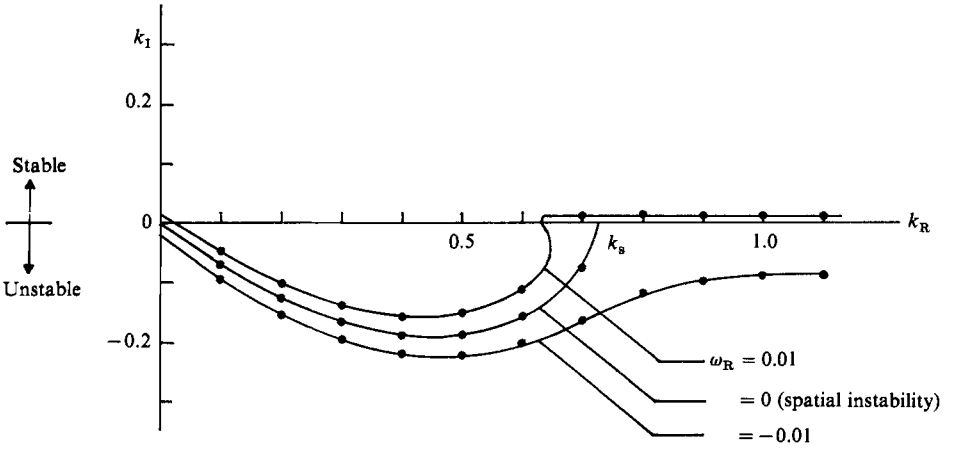

FIGURE 6. The curve of spatial instability for the infinitely differentiable profile; $R = 0.75$, $Re = 1.33 \times 10^4$, $U_m = 0.5$. ●, inviscid results for piecewise linear profile from (3).

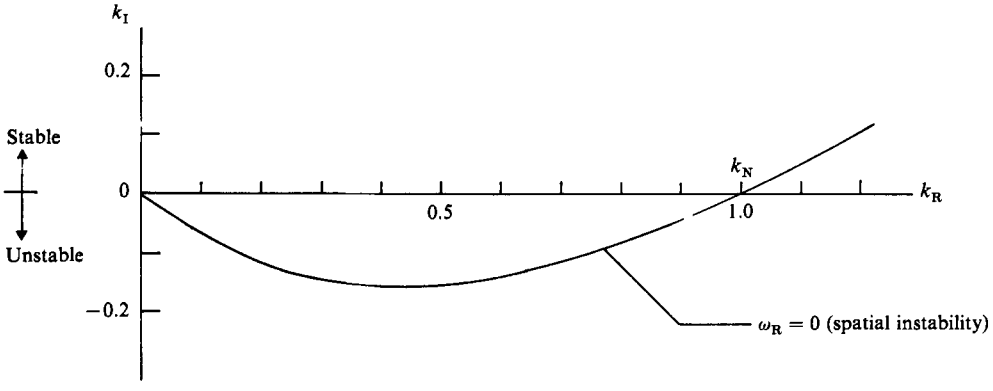

FIGURE 7. The curve of spatial instability for the tanh profile; $R = 0.75$, $Re = 1.33 \times 10^4$, $U_m = 0.5$.

Finally, in order to dramatically reinforce one of our principal conclusions, namely, that the inviscid spatial instability of the piecewise linear profile captures the viscous instabilities of an infinitely differentiable profile (which resembles the piecewise linear one) at large Reynolds numbers, we present figure 8. Note that the viscous calculations indicate that the spatially unstable mode becomes precisely neutral for frequencies larger than the neutral frequency, Ω_N. This is in exact agreement with the inviscid results for the piecewise linear profile.

In addition, in figure 8 we also show a qualitative comparison between the spatial growth rates of the tanh and piecewise linear profiles at a velocity ratio of 0.5. The two results are quite similar – the maximum spatial growth rates are about the same (they also occur at about the same frequency), although the range of frequencies for which the flow is unstable is narrower for the piecewise linear profile. The last remark is also completely consistent with the characteristics of the temporal stability of these two base flows and stems from the fact that, in the vicinity of $y = 0$, the piecewise linear profile is perfectly straight. As a side observation, we point out that free shear layers can be made stable at the higher frequencies by straightening the velocity profile near $y = 0$. (The significance of the point $y = 0$ has been mentioned already.)

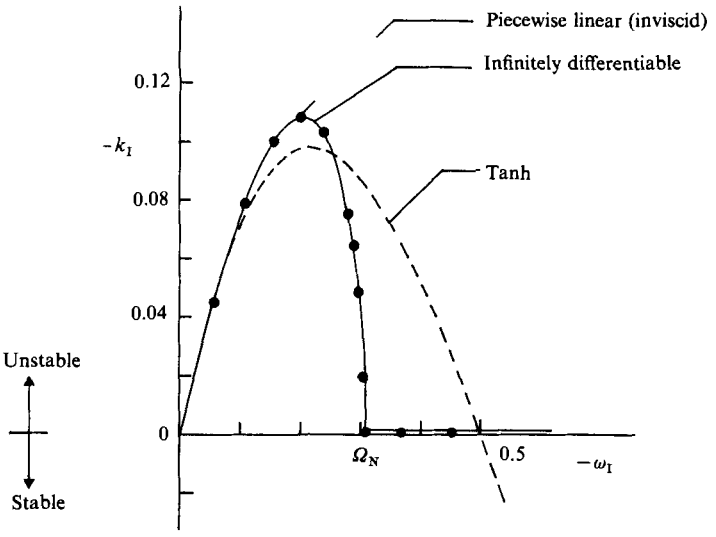

FIGURE 8. Spatial growth rate ($-k_I$) as a function of frequency ($-\omega_I$); $R = 0.5$, $Re = 1.33 \times 10^4$, $U_m = 0.5$. ●, Inviscid result for piecewise linear profile.

The dependence of spatial instability ($k_I < 0$) on velocity ratio is shown in figure 9. The main effect of increasing velocity ratio is to depress the curves (i.e. to increase the spatial growth rates) in both instances. The qualitative similarity between the spatial instability of the tanh and piecewise linear profiles is quite evident.

In addition to these obvious remarks, the results in figure 9(*b*) bring up a subtle point: Note that as the velocity ratio, R, increases, the intersection of the spatial instability curve with the branch cut, k_S, moves to the right. An important question is what happens to the spatial instability curve as k_S recedes to plus infinity (if this is indeed possible)? These remarks naturally lead us to the concepts of convective and absolute instability.

3.3 *Convective and absolute instability*

For $U_2 > 0$ (recall $U_1 \geqslant U_2$), the piecewise linear profile is convectively unstable. This means that a periodic excitation of the shear layer at frequency ω_I, for which the flow is spatially unstable, leads to a spatial instability mode as $x \to \infty$, $t \to \infty$. (For a more detailed discussion of convective and absolute instability, see Huerre & Monkewitz 1985.) On the other hand, when $U_2 = 0$, the velocity ratio is unity and the piecewise linear shear layer is absolutely unstable (Balsa 1986). In this case, a spatial instability mode can never arise in a properly posed initial-value problem which satisfies causality. For this case, the intersection point, k_S, is at plus infinity.

It is possible to show that whenever the piecewise linear profile is convectively unstable, the curve of spatial instability is unique there is only one curve at each velocity ratio; that curve is shown in figure 9(*b*). On the other hand, when the flow is absolutely unstable (say, $U_2 = 0$ or $R = 1$), there may be many curves of spatial instability. Some of these curves are shown in figure 10(*a*). The corresponding spatial growth rates, as functions of frequency, are given in figure 10(*b*), which is reproduced from Bechert (1972). The lowest branch in figure 10(*b*) corresponds to the uppermost curve of figure 10(*a*), and all the other branches correspond to each other in succession. The frequency varies from the value indicated (near the big dot) to 0.25 at infinity.

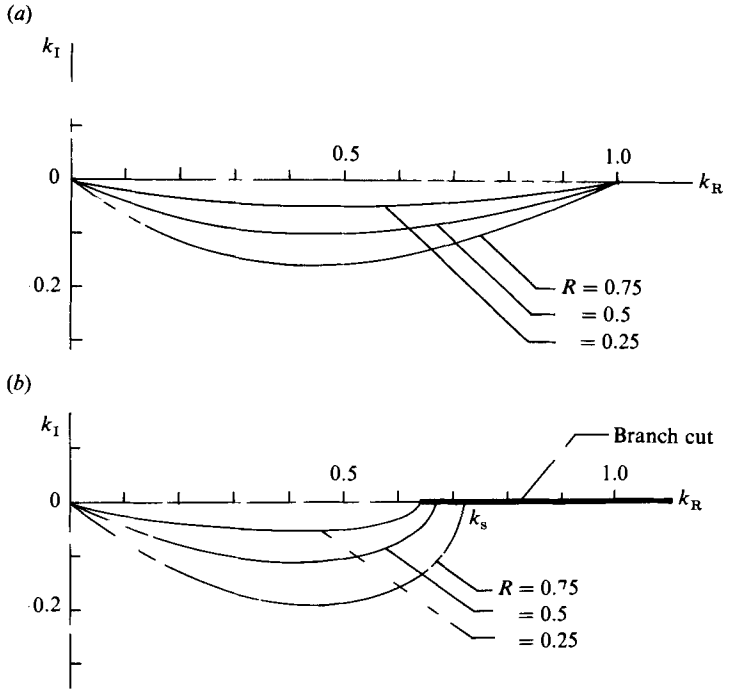

FIGURE 9. Dependence of spatial instability on velocity ratio (inviscid results, unstable range). (*a*) Tanh profiles; (*b*) infinitely differentiable and piecewise linear profiles.

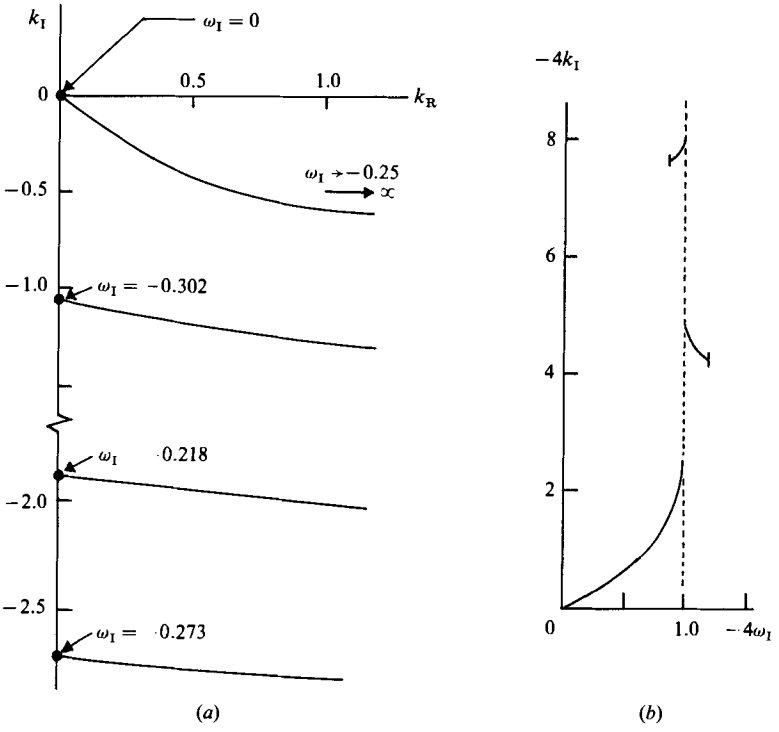

FIGURE 10. Non-unique spatial instability curves for an absolutely unstable piecewise linear velocity profile ($R = 1$) and the Bechert Christmas tree.

When figures 10(*b*) and 8 are compared, even qualitatively, it is clear that the results in figure 10(*b*) appear unphysical. Because of this, it is often claimed that the spatial instability of the piecewise linear profile is meaningless. This claim is wrong because it applies only in the situation where the shear layer is absolutely unstable, and in this case, spatial instability is meaningless in the context of a properly posed initial-value problem that satisfies causality. [A word of caution: Since the entire branch cut is part of the $\omega_R = 0$ curve only when $Re \to \infty$, one must be very careful about the limit process $Re \to \infty$ and $R \to 1$ (see figure 4). In order to retain our conclusions, it is best to say that $Re \gg 1$ and R is not too close to unity so that the spatial instability curve will indeed intersect the real axis.]

Spatial instability is meaningful only for convectively unstable flow ($0 < R < 1$). In this case, the spatial instability of the piecewise linear flow is quite acceptable on physical grounds and agrees extremely well with the viscous instability of the infinitely differentiable profile (figure 8). Any quantitative difference between the instability characteristics of the tanh and piecewise linear profiles is attributable to the fact that these profiles are not identical, though both are infinitely smooth.

4. Conclusions

We have shown through numerical solutions of the Orr–Sommerfeld equation that the temporal and spatial instabilities of our infinitely differentiable velocity profile at finite wavenumbers and very large Reynolds numbers (strictly as $Re \to \infty$) are virtually identical with those of the inviscid instabilities of a piecewise linear profile of Rayleigh. In particular, the unstable mode, upon passing through the neutral point, becomes exactly neutral rather than damped. This is undoubtedly due to the fact that the velocity profile in the vicinity of $y = 0$ is assumed to be perfectly straight.

Our results also show that the spatial instability of the piecewise linear profile is quite meaningful as long as the flow is convectively unstable. Furthermore, the conclusions of this paper reinforce an important point about spatial instability; namely, it is not enough to compute spatial growth rates without knowing how these fit into the complex dispersion relation $\omega = \omega(k)$ and the initial-value problem.

The author is grateful to NASA Lewis Research Center for financial support under Grant NAG 3-485.

REFERENCES

Balsa, T. F. 1986 On the receptivity of free shear layers (to be published).

Bechert, D. 1972 Über mehrfache und stromauf laufende Wellen in Freistrahlen. *DFVLR Rep.* DLR-FB 72-06.

Drazin, P. G. & Reid, W. H. 1982 *Hydrodynamic Stability.* Cambridge University Press.

Esch, R. E. 1957 The instability of a shear layer between two parallel steams. *J. Fluid Mech.* **3**, 289–303.

Huerre, P. & Monkewitz, P. 1985 Absolute and convective instabilities in free shear layers. *J. Fluid Mech.* **159**, 151–168.

Michalke, A. 1965 On spatially growing disturbances in an inviscid shear layer. *J. Fluid Mech.* **23**, 521–544.

Rayleigh, Lord 1945 *The Theory of Sound*, vol. 2. Dover.